SIR-C CALIBRATION RESULTS

A. Freeman, M. Alves, B. Chapman, J. Cruz, Y. Kim, S. Shaffer, J. Sun, E. Turner

Jet Propulsion Laboratory
California Institute of Technology

and

K. Sarabandi
University of Michigan

The SIR-C/X-SAR imaging radar took its first flight on the Space Shuttle Endeavour in April 1994 and flew for a second time in October 1994. This multi-frequency radar has fully polarimetric capability at L- and C-band, and a single polarization at X-band (X-SAR). The Endeavour missions were designated the Space Radar Laboratory -1 (SRL-1) and -2 (SRL-2). Calibration of polarimetric L- and C-band data for all the different modes SIR-C offers is an especially complicated problem, The solution involves extensive analysis of pre-flight test data to come up with a model of the system, analysis of in-flight test data to determine the antenna pattern and gains of the system during operation, and analysis of data from over fourteen calibration sites distributed around the SIR-C/X-SAR orbit track.

The SRL missions were the first time a multi-frequency polarimetric imaging radar employing phased array antenna has been flown in space. Calibration of S1 R-C data products involved some unique technical problems given the complexity of the radar system. In this paper, the approach adopted for calibration of SIR-C data is described and the calibration performance of the data products is presented.

Part of the work described in this paper was performed by the Jet Propulsion Laboratory, California Institute of Technology, under contract from the National Aeronautics and Space Administration.

I. INTRODUCTION

Calibration of data from imaging radar sytems is fast becoming a common feature of this type of data, rather than an exception. This is partly due to the individual and collaborative efforts of the members of the Committee on Earth Observing Sensors sub-group on SAR calibration [1], which has led to the routine availability of calibrated radar image data from the ERS- 1 [2] and JERS-1 [3] spaceborne radar systems, for example, and from airborne systems [4],

Calibration of radar image data from the Spaceborne Imaging Radar-C (SIR-C) data presented several unique technical challenges [5]. The SIR-C mission was the first time a multi-frequency, multi-polarization imaging radar system had been flown in space. The radar was designed and built to make eight different measurements at the same time: L.-Band (24 cm wavelength) and C-Band (6 cm wavelength) backscatter at four different polarization combinations, including horizontal transmit-horizontal receive (HH), horizontal transmit-vertical receive (HV), vertical transmit-horizontal receive (VH), and vertical transmit-vertical receive (VV). The SIR-C antenna ‘ an electronically steered, active phased array antenna which uses different electronic elements transmit and receive to boost the transmit power all across the array. This has the advantage that there is no single high-power transmission chain which can constitute a single point for failure, as happened on the earlier SIR-B mission [5]. A disadvantage from a calibration standpoint is that an active phased array antenna is not necessarily reciprocal like a passive antenna, i.e., the transmit beam patterns may not be the same as the receive beam patterns. The “ SIR-C antenna elements also showed a tendency to change their amplitude and phase characteristics with temperature. Since the orbit selected for the missions was not sun-synchronous, antenna temperature variations on the order of 40 degrees centigrade were anticipated. An additional calibration problem presented by the SIR-C antenna was the ability to electronically steer to 256 different beam positions, over a range of ± 20 degrees in elevation. The antenna provided another source of concern for calibration, in that the different beams needed to be aligned in elevation and azimuth in order to ensure that all channels were imaging the same area and to guarantee good correlation between the polarization channels at each frequency. The radar system had further complexities in that it operated using three different pulse bandwidths (10, 20 and 40 MHz) and three different pulse lengths, and was configured in 19 different data acquisition modes, which were combinations of the available frequencies and polarizations.

The SIR-C system and subsystems were extensively tested before flight, but the entire system had not been tested operating in a vacuum and over the range of temperatures expected in space. Thus a priority early in each mission was to demonstrate that the L-band and C-band radars were functioning properly as a polarimeters, and that the quality of the resulting images was within specifications. During both of the SIR-C/X-SAR missions in 1994, a number of SIR-C data-takes were downlinked to JPL and processed into full-resolution images. Several of these images were of sites containing calibration devices such as corner reflectors, transponders and ground receivers. The data from these sites was used to check out the system performance. Full-resolution data corresponding to these sites was calibrated and passed on to SIR-C science team investigators to perform real-time science during the missions.

Preparation for the missions included putting together a calibration workstation for analysis of the calibration performance of SIR-C data and for calibrating selected products. SIR-C investigators and their teams played their part in deploying the calibration equipment at fourteen of the SIR-C sites around the world and in sending the deployment data into JPL in a timely fashion. Over 150 corner reflectors, 70 transponders and 50 receivers were deployed at the calibration sites around the world. As a result, the first SIR-C data product was calibrated 31:20 hours into the April mission and 17 other image frames were calibrated during the mission. The first calibrated SIR-C image is shown in Figure 1. Following the first mission, the calibration team calibrated 35 image data-takes for investigators to analyze prior to the second mission. In

October, the first calibrated SIR-C image was generated 15:15 hours into the mission. SIR-C full-resolution image products generated by the Ground Data Processing Subsystem (GDPS) from Flight 1 were released as routinely calibrated in November 1994. Calibrated Flight 2 data were released early in February 1995.

Besides the analysis results provided by the calibration workstation, summary raw data quality analysis (QA) plots, showing range spectra, azimuth spectra, histograms and echo profiles of raw data, and histograms and amplitude/phase ratios generated from processed image data were produced by the Ground Data Processor team at JPL. Ground receiver measurements were also provided during the missions by investigators at DLR Oberpfaffenhofen, Race, Michigan and from the Institute for Navigation in Stuttgart, Germany.

In this paper, the calibration performance of the SIR-C system and the full-resolution image products is presented. The system model used in calibration is described in section II, results of our calibration analysis arc presented for SRI. -] in section 111, and for SRL-2 in section IV, followed by a summary and discussion in section V.

Figure 1. The first calibrated SIR-C image (L-Band, HH polarization). Over 30 corner reflectors and 6 transponders were deployed at this site in Death Valley, California

II. SYSTEM MODEI.

After [1], a convenient mathematical description of a complex SAR image is as follows:

$$V(x,y) = \sqrt{K_s}\, e^{j\phi_s}\, S_{pq}(x,y) \otimes h(x,y) + \sqrt{K_n}\, n_{pq}(x,y) \quad (1)$$

where V is the measured voltage, x and y are spatial position coordinates within the image, S_{pq} is the desired scattering matrix measurement for polarization p on transmit, q on receive, h is the impulse response function and $\otimes$ denotes convolution in both x and y. K_S and ϕs represent the gain and phase imposed by the radar on the backscatter measurement. $n_{pq}(x,y)$ represents the additive noise present in the backscatter measurements and K_n is the radar receiver and processor gain in the presence of noise.

A model for the behavior of Ks for each polarization/frequency combination was developed through pre-flight testing:

$$K_s = \frac{P_t G_t^A(\theta_{el},\theta_{az}) G_r^A(\theta_{el},\theta_{az}) \lambda^2 \; G_r^E G_p(x,y)}{(4\pi)^3 R^4 L_s L_a} \quad (2)$$

where P_t is the peak transmitted power; $G_t^A(\theta_{el},\theta_{az})$ and $G_r^A(\theta_{el},\theta_{az})$ are the antenna gains on transmit and receive, which change with elevation and azimuth angle θ_{el},θ_{az}; λ is the radar wavelength; G_r^E is the electronic gain in the radar receiver; L_s is a system loss term, included to account for attenuation due to cables, etc.; L_a is a loss term for propagation through the atmosphere (normally assumed zero for L-and C-band); R is the range delay; and G_p is the processor gain. Pre-flight testing of the antenna revealed that the antenna gains were a function of the antenna temperature and the bandwidth of the transmitted pulse, and were different for each polariz,ation/frequency. A model developed for the antenna also had to take into account any failures in the active electronic elements of the distributed ai ray and variations in the several hundred Transmit/Receive (T/R) modules used to drive the antenna. The receiver gain was also seen to be a function of the receiver temperature. During operation receiver gains were changed depending on the expected backscatter so that different gains were commonly used for like- and cross-polarized returns. To calculate the range delay, the electronic delay through the system (on transmit and receive) must first be removed: pre-flight tests revealed that this was a function of polarization, frequency and bandwidth.

During the SIR-C/X-SAR missions, sensors on the instrument were used to determine the temperature of the receivers and the antennas and the status of the active electronic elements of the distributed array. The dead-band on the space shuttle Endeavour was constrained to within ± 0.1 degrees, so that the on-board yaw, roll and pitch sensors could be used to obtain a reliable estimate for the mechanical pointing angle of the antenna, which was nominally 40 degrees off nadir (both left- and right-looking configurations were used during the missions). Other parameters used in the model for K_S were the electronic steering angle of the antenna, the radar polarization, frequency, the bandwidth used, the pulse repetition frequency, the pulse length and the mode of the radar operation for a given data-take. Pre-flight model analysis revealed that the variations of Ks in the along-track dimension (x) were negligible, so that only the range-dependent terms (y dimension) need be corrected for. Once an estimate for K_S is obtained as a function of range, a radiometric correction vector is applied to the measured voltages for each

polarization/frequency. This is done after SAR processing, i.e., radiometric correction is applied to the full-resolution complex image data.

From pre-flight testing and analysis, the major source of calibration uncertainty for SIR-C is the active, phased array antenna. Pre-flight tests showed that the antenna gain on transmit could change by - 1 dB over the expected range of operating temperatures during flight, while the antenna gain on receive could change by - 2dB. In addition, the electronic steering of the antenna and spoiling of the beam, in which a phase weighting is applied across the aperture to change the beam direction and shape, could result in large calibration errors, if not modeled properly. An example of two SIR-C antenna patterns is shown in Figure 2. The right-hand pattern in the figure corresponds to the L-band H-polarized pattern on transmit for zero degree beam steering and no spoiling, The left-hand pattern in the figure corresponds to the L-band H-polarized pattern on transmit for -10 degree beam steering and maximum spoiling.

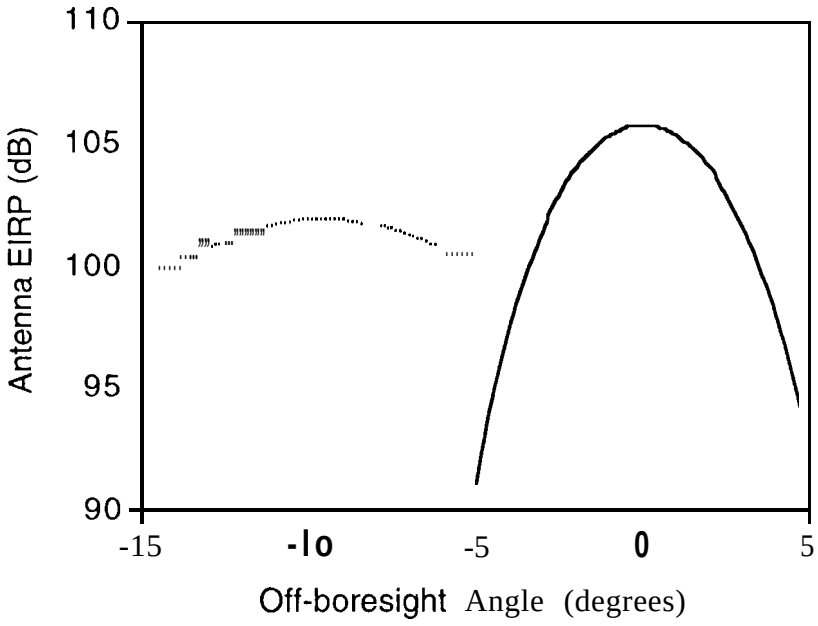

Figure 2: Example of two SIR-C transmit antenna patterns (L-band, H-polarization)

After radiometric correction, polarimetric measurements made by SIR-C can be modeled as follows:

$$\mathbf{M} = A\, e^{j\phi_s} \begin{pmatrix} 1 & \delta_1 \\ \delta_2 & f_1 \end{pmatrix} \begin{pmatrix} S_{hh} & S_{vh} \\ S_{hv} & S_{vv} \end{pmatrix} \begin{pmatrix} 1 & \delta_4 \\ \delta_3 & f_2 \end{pmatrix} + \frac{\sqrt{K_n}}{\sqrt{K_s}} \begin{pmatrix} n_{hh} & n_{vh} \\ n_{hv} & n_{vv} \end{pmatrix} \tag{3}$$

where A is a residual absolute calibration factor (ideally A should equal $1/(L_s L_a)$), the δ's are cross-talk terms, and f_1 and f_2 are channel balance terms. Ignoring the phase term, $e^{j\phi_s}$, and letting $n'_{pq} = \frac{\sqrt{K_n}}{\sqrt{K_s}} n_{pq}$, equation (3) can be expanded to give:

$$M_{hh} = A\left(S_{hh} + \delta_2 S_{hv} + \delta_4 S_{vh} + \delta_2\delta_4 S_{vv} + n'_{hh}\right) \quad (4a)$$

$$M_{hv} = A\left(d_1 S_{hh} + f_1 S_{hv} + \delta_1\delta_4 S_{vh} + f_1\delta_4 S_{vv} + n'_{hv}\right) \quad (4b)$$

$$M_{vh} = A\left(\delta_3 S_{hh} + \delta_2\delta_3 S_{hv} + f_2 S_{vh} + f_2\delta_2 S_{vv} + n'_{vh}\right) \quad (4C)$$

$$M_{vv} = A\left(\delta_1\delta_3 S_{hh} + f_1\delta_3 S_{hv} + f_2\delta_1 S_{vh} + f_1 f_2 S_{vv} + n'_{vv}\right) \quad (4d)$$

To complete the calibration of any measurement M_{pq}, for each frequency, the cross-talk terms (the δ's) need to be estimated and corrected for if they are significant, the cross-polarized measurements must be symmetrized such that HV = VH, the HH, HV and VV measurements must be balanced in amplitude and phase, and the absolute calibration must be completed. For fully polarimetric data, an approach described in [7] was adopted, in which the assumption of backscatter reciprocity (i.e. $S_{hv} = S_{vh}$) is used to estimate the ratio f_1/f_2, which is then applied to the VH and VV measurements as a multiplicative factor to symmetrize the data and remove any imbalances in amplitude and phase between the cross-pol channels. Then assuming azimuthal symmetry in the scatterers, it is possible to estimate and correct for any system cross-talk. The remaining channel amplitude and phase balance (related to f_1 and f_2) and absolute calibration (A) terms were estimated using selected data-takes containing trihedral corner reflectors. This approach relies on a certain, degree of stability in the system, and assumes that most of the variations due to using different bandwidths, pulse lengths, receiver gains, modes and operating temperatures are correctly removed during radiometric correction (for K_S).

For single- or dual-polarization data, for which all four channels were. not available, it was assumed that the cross-talk was negligible, then channel amplitude and phase balance and absolute calibration corrections were applied using parameters estimated from selected data-takes containing trihedral corner reflectors.

In calibrating the data from SIR-C, the following performance goals were established (after [8]):

TABLE 1. SIR-C Calibration Performance Goals

Parameter	Goal
Absolute calibration	± 3.0 dB
Short-term relative calibration [1]	± 1.0 dB
Long-term relative calibration	± 1.5 dB
Channel amplitude balance	± 0.4 dB
Channel phase balance	± 10 degrees
Cross-talk	< - 30 dB

1. **i.e. within an image frame**
2. **i.e. from pass-to pass over the** same **site**

III. SRL-1 RESULTS

A. *Raw Data Analysis*

Analysis of the Quality Assurance (QA) plots generated from SIR-C data initially focused on whether the different 'polarization channels at-each frequency were behaving the same and whether the different beams for each polarization were pointing in the same direction. Doppler spectra estimated from the raw data were compared with preflight antenna model predictions, converting azimuth angles to Doppler frequency. Conclusions drawn from this analysis were:

1. For each frequency, the HV and VH range spectra, azimuth spectra, histograms and echo profiles of raw data, and histograms of processed image data appeared identical, which gave a good indication of system reciprocity, i.e. that the behavior of the antenna on transmit and receive was similar.

2. The Doppler Spectra indicated that all beams for a given frequency were pointing in the same directions. The normalized Doppler spectra power values went from O to -10 dB over a range of -150 Hz which matched predictions from the preflight SIR-C antenna model.

3. Range spectra were consistent with preflight test results. In particular, the pulse bandwidths were within specifications for 10, 20 and 40 MHz data-takes.

4. During the first mission, initial analysis of ratios of HH/VV and HV/VH amplitude and phase from image data indicated that the polarization channels were not registered. Large variations in the HV/VH amplitude and phase in particular were strong indicators of this. This was immediately fixed in the processor once the appropriate offsets between the polarization channels had been determined by analysis of calibration device signatures.

B. *Ground Receiver Measurements*

Several teams of investigators made field measurements of the SIR-C/X-SAR transmit antenna patterns with ground receivers. These results were transmitted to the calibration team at JPL during the missions. The analysis of these results was given added significance since it was known from the built-in test capability of the SIR-C antenna that one of the 18 C-band panels had failed early on during SRL-1 and that 2 C-Band panels partially failed during SRL-2. A summary of what was found is contained in Table 2.

These results are consistent with expectations from pre-flight measurements. These results indicated that the SIR-C beam shapes were as expected for both L-band and C-band, that the H and V beams were coaligned and that the beams from L-band, C-band and X-band were sufficiently coaligned in both elevation (El.) and azimuth (Az.). The pointing of the C-Band antenna was found to be off by 0.35 degrees in elevation from measurements at the DLR site - this was later confirmed by analysis of images over tropical rain forest sites.

TABLE 2: Summary of Ground Receiver Measurements

Measurement	L-Band	C-Band
3 dB Azimuth Beamwidth	1.0^{o}	0.22^{o}
Mainlobe width (null-null)	2.3^{o}	0.5^{o}
Azimuth PSLR	-12.8 dB	-10.4 dB
H-V beam alignment (Az.)	Yes	<4% of 3dB BW
H-V beam alignment (El.)	0.2^{Θ}	0.3^{Θ}
L,X Alignment (Az.)	<13% of X 3dB BW	-
L,X Alignment (El.)	0.5^{o}	-
L,C Alignment (Az.)	-	<11% of C 3dB BW
L,C Alignment (El.)	-	0.6^{o}
C,X Alignment (Az.)	-	<27% of X 3dB BW
C,X Alignment (El.)	-	0.5^{o}
3dB El. Beamwidth	4.8^{o}	4.7^{o}

C. Image Quality

A sample of a SIR-C impulse response function is shown in Figure 3. The target used to obtain this response was one of the high-precision C-band transponder deployed at the Flevoland site in the Netherlands by our colleagues from FEL-TNO and the European Space Agency at ESTEC. Measurements made of the impulse response function derived from analysis of corner reflector signatures in several scenes (Table 2) showed that the resolution and PSLR were well within the specifications for both 10 MHz and 20 MHz bandwidths. ISLR measurements are close to the goals, but have larger variations due to measurement error.

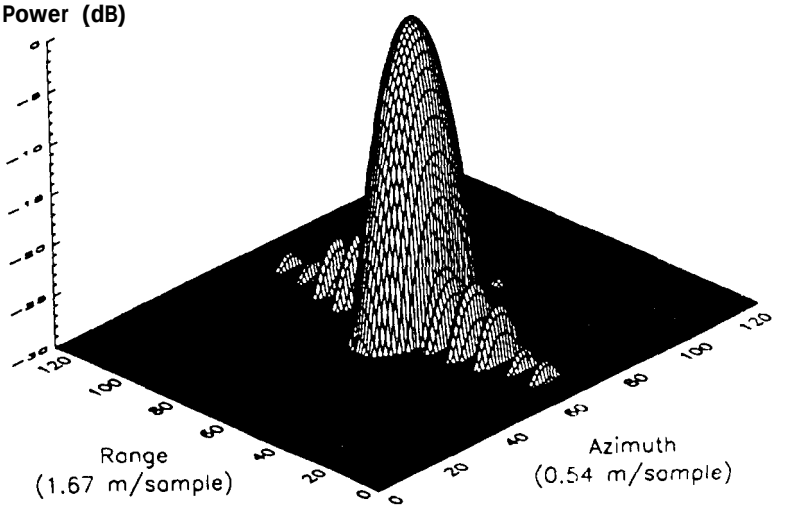

Figure 3: Impulse response function from SIR-C data.

TABLE 3: Summary of Image Quality results

10 MHz Results	L-Band	C-Band	Goal
Range Resolution (m)	14.9(*2.9)	14.5~) —	< 18.0
PSLR (dB)	-17.2(±2.1)	-17.2(*2.9)	<-17
ISLR (dB)	-13.0(±2.2)	-16. 0(±0.9)	<-14
Azimuth Resolution (m)	7.6(±0.9)	7.7(±0.8)	Variable
PSLR (dB)	-21.3(±3.9)	-22.8(±3.7)	<-17
ISLR (dB)	-12.2(*4.7)	-13.7(*4.7)	<-14

20 MHz Results	L-Band	C-Band	Goal
Range Resolution (m)	8.3(±0.3)	7.9(*0.3)	< 9.0
PSLR (dB)	-17.8(±3.2)	-15.6(±4.6)	<-17
ISLR (dB)	-15.0(±1.0)	-14.2(±2.0)	<-14
Azimuth Resolution (m)	8.0(±1.1)	8.0(±1.1)	Variable
PSLR (dB)	-18.0(±2.0)	-22.0(±3.0)	<-17
ISLR (dB)	-14.0(±1.0)	-12.8(±4.5)	<-14

Numbers in parentheses in Table 3 are the range of values over many data-takes. The azimuth resolution varies with the processing bandwidth which depends on the PRF selected. These results are consistent with pre-flight test results. Analysis of transponders (which have a very high signal-to-background ratio) at the Flevoland site indicates that the ISLR and PSLR'S were actually considerably better than the goals. 40 MHz data over the Flevoland site was also analyzed and shown to have achieved 4m resolution in (slant) range plus good impulse response quality.

The interpolated peak positions of corner reflector and transponders were used to check the registration between the different polarization and frequency images. After some initial iterations of the SIR-C processor, the HH, HV, VH and VV channels were shown to be registered at both frequencies to within the limits of our measurement capability (which is +/- 1/8 of a pixel). Confirmation that the polarization channels are registered in SIR-C data was provided by measurements of the correlation coefficient between the HH and VV polarizations over water, and between HV and VH polarizations over forested areas, which were close to 1, as expected. Analysis of reflector signatures showed that the different frequencies were registered to better than the goal of 1/2 pixel.

D. Radiometric Correction

Many SIR-C images have now been calibrated using the system model described in section II. Initial analysis focused on whether the preflight elevation antenna pattern matched that of the actual data and what residual cross-swath radiometric uncertainties remained after the nominal radiometric correction had been applied. To answer these questions, S1 R-C data from several uniform tropical rain forest scenes were analyzed after radiometric correction had been applied. Residual ranges of variation (peak-to-peak excursions) in the range dimension for rain forest data are given in Table 4.

TABLE 4: Residual variations in estimated backscatter for a uniform tropical rain forest scene

	HH	VV	HV
L-Band	±0.35 dB	±0.6 dB	±0.4 dB
C-Band	±0.25 dB	±0.25 dB	±0.25 dB

These results are better than the goal of ± 1 dB for SIR-C data. These results were verified by analysis of other scenes with uniform scatterers and scenes with a large number of reflectors distributed across them. A few exceptions were found for wh[illegible] calibration uncertainties were greater than those quoted above. These are as follows:

1. Uncertainies in the shuttle roll angle on the order of 0.1 -0.2 degrees mean that some scenes may have residual cross-track radiometric errors of ± 1 dB.

2. Data-takes for which the electronic steering angle exceeded 17.5 degrees on either side of the mechanical antenna boresight or wide swath data-takes for which the data extends to off-boresight angles greater than 17.5 degrees. Outside the range of electronic steering angles between +17.5 and -17.5 degrees the model of the SIR-C antenna pattern appears to break down, leading to large cross-swath radiometric errors (of several dB).

3. In processing, a constant scene altitude is assumed in order to determine the pointing angle of the antenna. If this altitude is in error, or the terrain height varies significantly within the scene (e.g.)in going from a coastal plain at or near sea level to a mountain range at high elevation)'significant cross-swath radiometric errors may result [9].

Two Amazon scenes separated by a few seconds in the mission timeline were also analyzed. The results showed that both the L-band and C-band radars were stable over this timeframe and the processor contribution to the calibration error was <0.3 dB.

E. Polarimetric Calibration

After radiometric correction, the next step in calibration of SIR-C fully polarimetric data is symmetrization. Within any single image, the variations across the image in range of the HV/VH ratio were seen to be less than ±0.3dB in amplitude, ±3 degrees in phase. This verified that the radar antenna was very nearly reciprocal, which means that the transmit and receive patterns for a given polarization were very similar. This applied to both L-band and C-band.

Radiometric correction did not remove the channel imbalances between HV and VH polarizations entirely. Residual values for the amplitude and phase balance between the cross-pol channels are given in Table 5.

TABLE 5. Residual values for HV and VH channel imbalances

Amplitude (dB)	L-band	C-band
10 MHz	-0.4 (± .2)	q - z j - - -
20 MHz	-0.7 (± .2)	-1.9 (± .1)

Phase (degrees)	L-band	C - b a n d
10 MHz	66 (± 2)	183 (± 6)
20 MHz	45 (± 4)	169 (± 5)

The values in parentheses are the observed range of variation in the cross-pol channel imbalances over the first mission. These residual variations are well within the goals from Table 1 of ±0.4 dB and ± 10 degrees. Plots of typical channel imbalance values for C--band arc given in Figure 4 (the L-band results are similar). The plots show the results as a function of electronic steering angle clustering into two populations for 10 and 20 MHz bandwidths. [Note: The *mechanical* steering angle for the SIR-C antenna was nominally 40 degrees off nadir, so that an *electronic* steering angle of O degrees corresponds to a look angle of 40 degrees off nadir. To maximise swath width while keeping the range resolution reasonably high, most SIR-C data-takes with a

look angle of less than 36 degrees had 20 MHz bandwidth: those with a look angle greater than or equal to 36 degrees had 10 MHz bandwidth.]

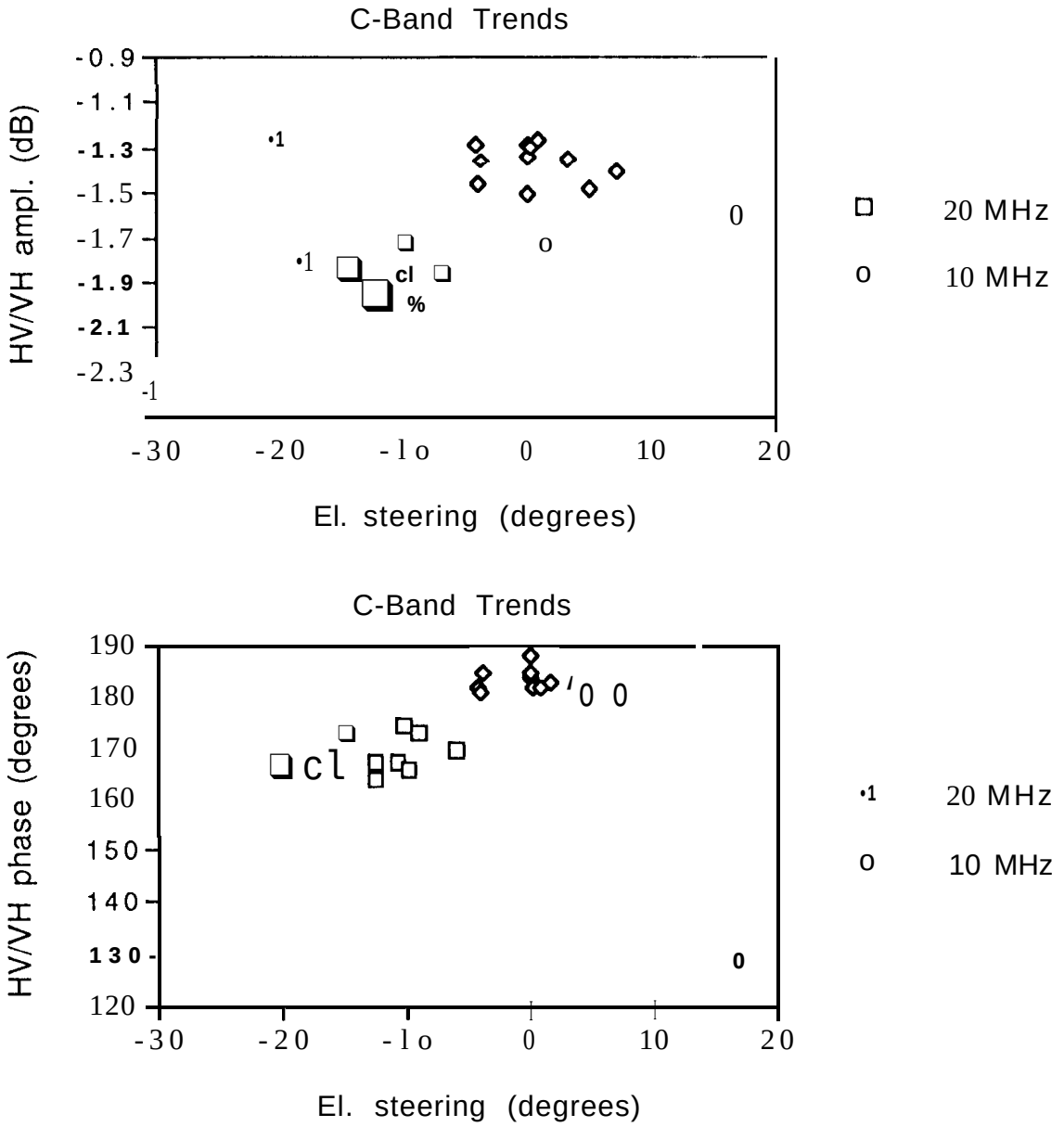

Figure 4: HV/VH amplitude variations for different electronic steering angles

It was noticeable that for large electronic steering angles (i.e. >±17.5 degrees) the HV/VH channel imbalances were significantly different at both frequencies.

For some data-takes, the algorithm implemented to estimate the channel imbalance between the cross-pol measurements did not converge. This occurred for data-takes over the ocean and some desert areas, where the cross-pol backscatter was very low.

Cross-talk values estimated using the algorithm described in [10] from fairly uniform scenes showed that the cross-talk was uniform across a given image. An examination of the average cross-talk value for several different steering angles revealed that the cross-talk was always better than the performance goal of -30 dB (see Figure 5).

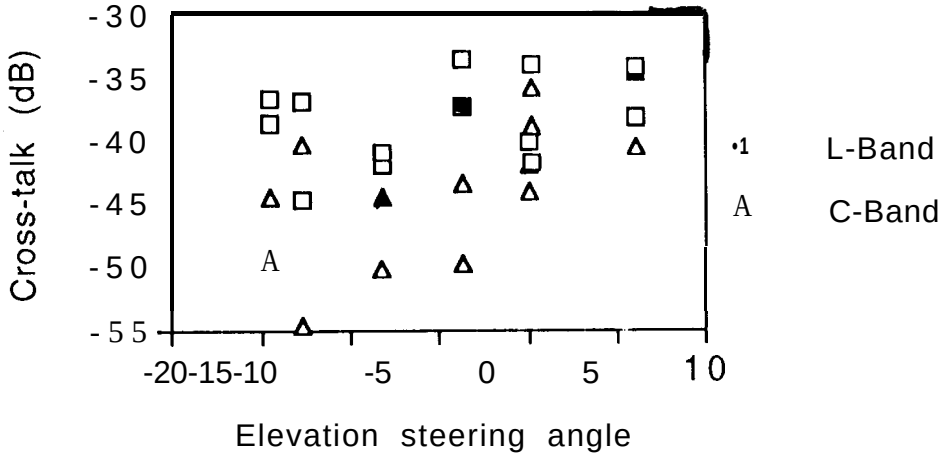

Figure 5: Average cross-talk estimates vs. elevation steering angle

After symmetrization, initial analysis of data obtained over some fairly uniform distributed targets revealed a variation of 1-2 dB in the HH/VV amplitude ratio across an image for L-band 20 MHz data. Analysis of a long data-take over the Amazon revealed that variations over a few minutes in the HH/VV channel imbalances were negligible. Further investigation of the L-band 20 MHz data indicated that the H and V beams were misaligned by -0.2 degrees, which was confirmed by ground receiver measurements, then corrected in the antenna pattern model used for radiometric correction. (An observed 0.3 degree misalignment between H and V at C-band was already incorporated into the antenna pattern model.) After this change, residual cross-swath variations for both frequencies and at both bandwidths were observed to be less than ± 0.4 dB (peak-to-peak). A summary of the HH to VV channel imbalances subsequently analyzed from corner reflector signatures at a number of sites is given in Table 6.

TABLE 6. Residual values for HH and VV channel imbalances

Amplitude (dB)	L-band	C-band
10 MHz	-0.3 ($\pm$ .7)	-3.3 ($\pm$ .5)
20 MHz	-1.1 ($\pm$ .4)	-4.1 ($\pm$ .6)

Phase (degrees)	L-band	C-band
10 MHz	-48 ($\pm$ 5)	180 ($\pm$ 4)
20 MHz	-49 ($\pm$ 5)	167 ($\pm$ 4)

The values in parentheses are the observed range of variation in the like-pol channel imbalances over the mission. These residual variations are just outside the goal of $\pm$ 0.4 dB for the amplitude balance and well within the goal of $\pm$ 10 degrees for the phase imbalance. The results for different electronic steering angles again clustered into two populations for 10 and 20 MHz bandwidths. No dependence on time of data acquisition was apparent in the data. For large

electronic steering angles (i.e., >±17.5 degrees) the HH/VV channel amplitude imbalances were significantly different at both frequencies. There was particularly pronounced effects in the case of the HH/VV phase difference at C-band (see Figure 6). On further investigation, it was discovered that the HH/VV phase difference at C-band for electronic steering-angles greater than 17.5 degrees in towards nadir had a significant, approximately linear variation in range across the image, from -123 degrees at near range to - 167 degrees at far range.

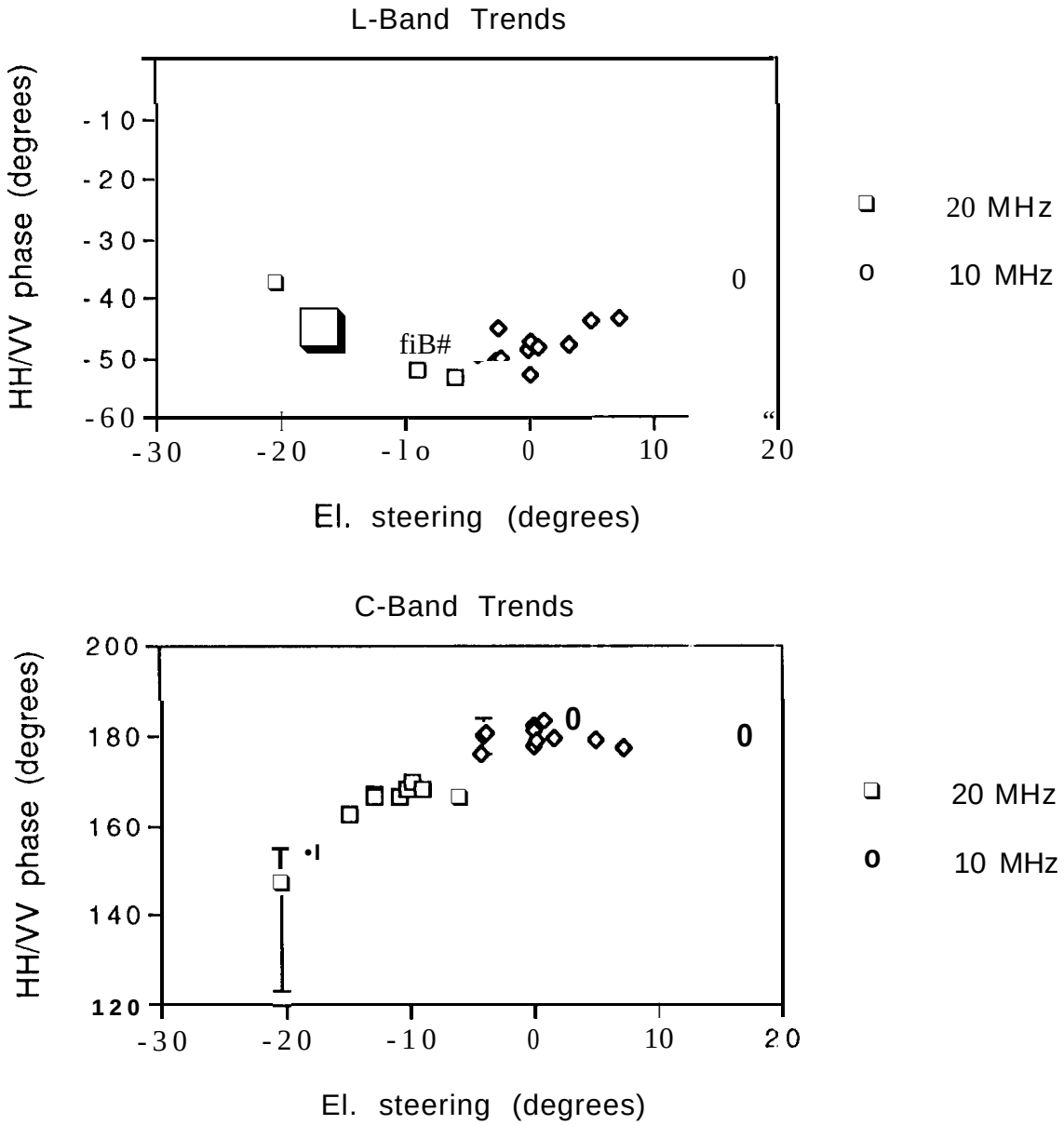

Figure 6: Plots of average HH/VV phase differences vs. electronic steering angle

F. Absolute Calibration

After radiometric correction, syrnmetrization and channel balancing, the residual gain variations [i.e., the variations in the parameter A from equation (4)] were estimated by comparing the theoretical radar cross section for trihedral corner reflectors with measured values for a number of data-takes at selected sites, using both the integrated and peak methods for analyzing reflector responses [11]. The results are summarized in Table 7 and plotted as a function of steering angle in **Figure** 7. In the normal calibration procedure, the average values for A given in Table 7 are applied to the data.

TABLE 7. Residual gain variations (absolute gain, A)

Amplitude (dB)	L-band	C-band
10 MHz	-3.1 (± 1.3)	-0.7 (± 1.2)
20 MHz	-0.7 (± 1.3)	-0.2 (± .9)

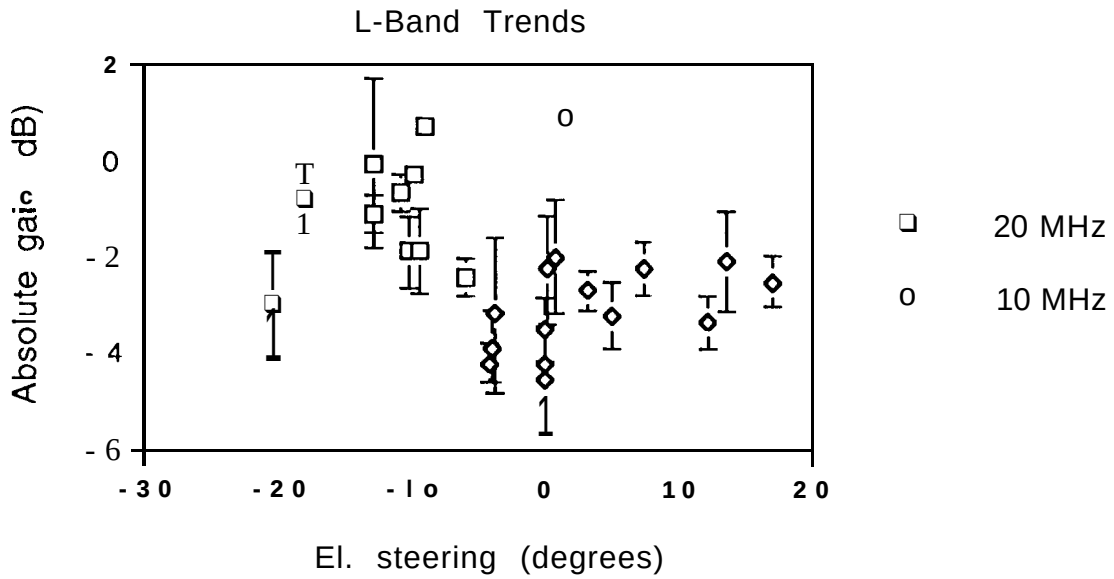

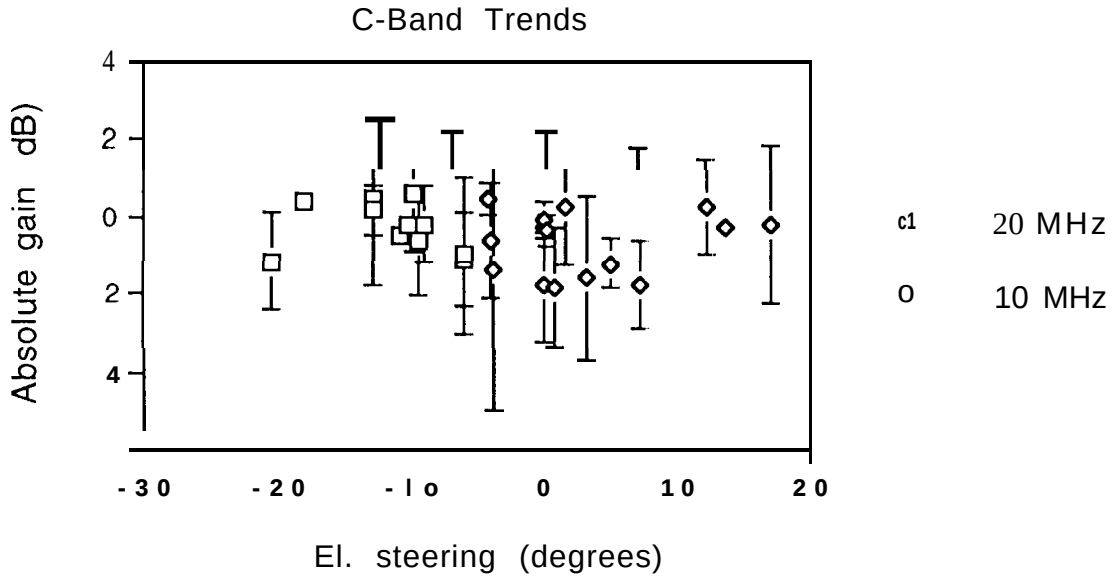

Figure 7: Plots of residual absolute gain versus electronic steering angle

Values given in parentheses in Table 7 are peak-to-peak variations over the mission, which are within the goal of ±1.5 dB. The error bars shown in Figure 7 are rms variations for a given data-take. There was considerably more variation in the L-band results than for C-band. Some of the variation seen in the figure can be attributed to corner reflector misalignment or imperfections. Results for large steering angles are within the range of variation for other steering angles. No significant trends in residual gain versus data acquisition time during the mission were apparent,

Image Noise Levels

The noise level or noise-equivalent sigma-zero in SIR-C' data is variable and depends on a number of factors. Most data-takes collected were in (8,4) bit Block Floating-point Quantization (BFPQ) mode [12]. In BFPQ mode a 'block' of data is first quantized to 8 bits then re-quantized to give the optimum 4-bit representation of that block of data. This approach gives a fairly large dynamic range, for relatively few bits per sample, and avoids the problem of saturation during analog-to-digital conversion, which can be a significant source of calibration error [2]. In this case the quantization noise is always - 18 dB down on the average signal power for that 'block' of data. Thus, considering quantization noise alone, if a patch of forest has a σ^o of -10 dB, a nearby patch of smooth water, with very low backscatter may have an image power level of about -28 dB. Of course, thermal noise enters into the calculation too, as does the range attenuation of the signal (which will vary significantly depending on the look angle). In one case, we have measured the noise-equivalent sigma-zero to be -50 dB for LHV and -35dB at C-band for a data-take over the Sahara Desert, which is consistent with the predicted system performance for that particular data-take. More typical values estimated from cross-pol measurements over smooth water secm to hover around -28 dB for C-band and -36 dB for I.-band. Again, this depends on the set-up of each data-take.

IV. SRL-2 RESULTS

In this section, a summary of the results of our calibration analysis of data from SIR-C during SRL-2 is given, For Flight 2, data from twenty calibration site data-takes were analyzed. Overall, the calibration results are very similar. Only those results which are significantly different from SRL-1 will be discussed.

Slight differences were found in the absolute gain at both L-band and C-band, for 10 and 20 MHz data. The trend was for the signal strength to be lower for Flight 2 data. The worst case was for L-band 20 MHz data, which exhibited a drop in gain of 1.6 dB. The C-band 20 MHz data dropped by 1.1 dB, and the L- and C-band 10 MHz data both dropped in gain by less than 1 dB. Variations in the absolute gain between data-takes was found to be higher at C-band for Flight 2 data.

The symmetrization parameter, which is an estimate for the channel balance between HV and VH measurements showed significantly larger variations (± 0.3 dB instead of ±0.2 dB at L-band, ± dB instead of ±0.2 dB-at C-band).

The HH-VV phase difference, estimated from corner reflector signatures, showed slightly larger variation for Flight 2 data, but was still less than 10 degrees over all data-takes analyzed.

V. SUMMARY AND DISCUSSION

The image quality at all three bandwidths for SIR-C was better than or very close to the goals for the mission. The different polarization channels were fully registered in the image data products. The in-flight antenna pattern was found to be consistent with the pre-flight measurements and the antennas were shown to be very nearly reciprocal (i.e., transmit beam pattern has the same shape as the receive beam pattern) for each polarization/frequency combination. Calibration results fell into two populations: one at 20 MHz, or for look angles less than 36 degrees; and one at 10 MHz, or for look angles greater than or equal to 36 degrees. Not enough 40 MHz bandwidth data was collected or analyzed to say whether the 40 MHz data constituted a third grouping.

To summarize the steps involved in calibration of SIR-C data:

1. After processing a radiometric correction vector is applied to the complex image data corresponding to each channel.

2. For quad-pol data, the next step is to calculate the symmetrization parameter, which is then applied to the VH and VV channels to symmetrize the data.

3. The HH and VV channels are balanced in amplitude and phase by applying a standard correction factor (from Table 6).

4. The absolute calibration is completed by applying one of the standard gains from Table 7

For single-pol or dual-pol data, standard values from Tables 5, 6 and 7 are used to balance the polarization channels, and complete the absolute calibration. For a VV only measurement, for example, a 'standard' symmetrization factor, an HH-VV channel balance and an absolute calibration factor are applied to the data. For an HH measurement, only the absolute calibration factor is applied.

Calibration uncertainties were found to be significantly worse at extreme electronic steering angles in elevation, i.e., greater than 17.5 degrees either side of the mechanical boresight. There appear to be two explanations for this: firstly, the antenna model developed for SIR-C does not appear to match the actual pattern very well at large steering angles; secondly, at small incidence angles, data-takes tended to be widened to include returns from outside the 2-way 6-dB points of the antenna pattern (because the signal strength was high enough to allow this). Collecting data from areas illuminated by the steeply varying portion of the antenna main lobe in this fashion increases the calibration uncertainty.

Both the L-band and C-band radars were demonstrated to be fully operational as polarimetric systems and the cross-talk between polarization channels at both frequencies was found to be below the goal of -30 dB. Thus cross-talk removal based on the ensemble properties of distributed targets [11] is unnecessary - the system performance is already good enough. The system was shown to be phase stable to within a few degrees, as far as the phase difference between polarizations was concerned. The channel amplitude balance between the cross-pol (HV and VH) measurements was shown to be consistent to within a couple of tenths of a dB. The amplitude balance between the like-pol (HH and VV) measurements was close to the goal of being calibrated to within 0.5 dB.

When cross-pol backscatter is very low, the symmetrization algorithm applied to the quad-pol data to calculate the channel balance between the HV and VH measurements sometimes fails to converge or converges to a 'wrong answer'. This is because ambiguities from the like-pol channels tend to dominate the signal in the cross-pol channels. Typical azimuth ambiguity ratio levels for SIR-C are estimated at around -20dB (though some data-takes should be significantly

better than this). Thus if the cross-pol backscatter is 20 dB below the like-pol, ambiguities may dominate in the cross-pol data. The solution adopted is to check for non-convergence in the symmetrization or for symmetrization parameters which are very different from the values in Table 5. In these cases, the symmetrization parameters used are the default values, i.e those given in Table 5.

To balance the HH and VV channels, the average amplitude and phase imbalances over the mission given in Table 6 were applied to the data. This left residual variations in the channel phase imbalances which were within the goals but residual amplitude imbalance variations which were just outside. It is not clear whether the cause of these residual amplitude balance variations is the SIR-C system itself or errors in the measurements (from corner reflector signatures).

Phase calibration and amplitude balancing were observed to break down at extreme steering angles for C-Band. The behavior of the phase difference between HH and VV, which has a linear ramp on it across range in some images, is consistent with an offset between the H and V antenna phase centers of about 2λ, or 11.2 cm, after [13]. Close to boresight the phase variation introduced by this offset is very small. But at around 17-20 degrees off boresight it becomes significant.

Over a relatively flat, uniform area, it was shown that the residual cross-track amplitude variations were small. The processor contribution to calibration uncertainties was found to be small. The absolute calibration results suggest that the system model matched the actual behavior of the SIR-C system quite well (to within -4 dB at least). No obvious trends in the absolute gain versus Mission Elapsed Time (MET) were apparent, which suggests that any effects due to the variation in antenna temperature of 30 degrees centigrade over SRL- 1, for example, were tracked successfully by the antenna pattern generation model used to calibrate the data. The strategy adopted for absolute calibration was to apply the residual gains given in Table 7 to the data after radiometric correction, symmetrization and channel balancing.

After applying the 'standard' corrections from Table 7, the observed variation in residual system gains are within the goal of $\pm$1.5 dB, except for C-band data in Flight 2. This allows for an error margin of $\pm$1.7dB in the theoretical versus actual radar cross section of the corner reflectors used at the SIR-C calibration sites. This error margin is consistent with measured variations in theoretical versus actual RCS for the JPL design corner reflectors, as determined from pre-flight measurements of their RCS.

The estimated residual calibration uncertainties for Flight 1 data, obtained by analyzing calibration results for over thirty SIR-C scenes, are given in Table 8.

TABLE 8: Calibration uncertainties for SRL- 1 data

	L-Band	C-Band	Goal
Absolute Calibration	$\pm$2.3 dB	$\pm$2.2 dB	$\pm$3.0 dB
Cross-swath calibration	$\pm$1.0 dB	$\pm$1.0 dB	$\pm$1.0 dB
Pass-to-pass calibration	$\pm$1.3 dB	$\pm$1.2 dB	$\pm$1.5 dB
HH/VV amplitude imbalance	$\pm$0.7 dB	$\pm$0.6 dB	$\pm$0.4 dB
HV/VH amplitude imbalance	$\pm$0.2 dB	$\pm$0.2 dB	$\pm$0.4 dB
HH/VV phase imbalance	$\pm$5 deg.	$\pm$4 deg.	$\pm$10 deg.
HV/VH phase imbalance	$\pm$2 deg.	$\pm$6 deg.	$\pm$10 deg.
Cross-talk	<-33 dB	<-35 dB	< -30 dB

Calibration analysis results and uncertainties for Flight 2 data were very similar to those obtained for Flight 1 data, with the exception of the absolute gain values, the symmetrization parameter

and the short-term variations in gain at C-band. Calibration uncertainty results for Flight 2 data are given in Table 9.

TABLE 9: Calibration uncertainties for SRL-2 data

	L-Band	C-Band	Goal
Absolute Calibration	±2. dB	±3.2 dB	±3.0 dB
Cross-swath calibration	±1.0 dB	±1.0 dB	±1.0 dB
Pass-to-pass calibration	±1.0 (1B	±2.2 dB	±1.5 dB
HH/VV amplitude imbalance	±0.7 dB	±0.6 dB	±0.4 dB
HV/VH amplitude imbalance	±0.3 dB	±0.5 dB	±0.4 dB
HH/VV phase imbalance	±9 deg.	±5 deg.	±10 deg.
HV/VH phase imbalance	±3 deg.	±4 deg.	±10 deg.
Cross-talk	<-33 dB	< -35 dB	<-30 dB

There are exceptions for which the calibration uncertainties may be greater than those quoted above in Tables 8 and 9. These arc:

1. **Data-takes** for which the electronic steering angle exceeded 17.5 degrees on either side of the nominal antenna boresight or wide swath data-takes for which the data extends to off-boresight angles greater than 17.5 degrees. These data-takes mav have large cross-swath radiometric errors, channel amplitude balance and phase calibration errors.

2. In processing, a constant user-supplied scene altitude is assumed in order to determine the pointing angle of the antenna. If this altitude is in error, or the terrain height varies significantly within the scene (e.g. in going from a coastal plain at or near sea level to a mountain range at high elevation) significant cross-swath radiometric errors may result. This will be the subject of a future paper.

3. Data-takes with strong interference signatures may have large calibration errors.

With the exceptions noted above, SIR-C data products, whether in single-look complex (scattering matrix) or multi-look complex (covariance matrix) format, are now fully calibrated to within the uncertainty levels given in Tables 8 and 9.

ACKNOWLEDGMENTS

The SIR-C calibration team would like to express our heartiest thanks to all those within the SIR-C project at JPL, the SIR-C investigators and their teams and our colleagues from the CEOS Sub-Group on SAR calibration who helped us to calibrate his complex radar system. We would particularly like to thank Manfred Zink of DLR Oberpfaffenhofen, Jos Groot, Bert van den Brock and Peter Hoogeboom of FEL-TNO in the Netherlands, Geoff Taylor, John Richards and their team in Australia for their efforts in helping to calibrate SIR-C. In our deployments at the Death Valley site we were greatly aided by Dr. Dan Blumberg and his team from Arizona State University, and by the helpful cooperation of Ranger Dick Anderson of the National Park Service. Finally, we would also like to thank Dr. John Curlander (formerly of JPL, now Vexcel Corporation) for having the foresight to stress SIR-C calibration from the early days of the project.

REFERENCES

[1] Freeman, A., SAR Calibration: An Overview, IEEE Trans. on Geoscience and Remote Sensing, Vol. 30, No. 6, pp. 1107-1121, November 1992.

[2] Laur, H., Sanchez, J., Dwyer, E. and Meadows, P., ERS-1 SAR Calibration, Proc. of the 1993 SAR Calibration Workshop, ESA WPP-048, ESTEC, Noordwijk, The Netherlands, pp. 257-281, September 1993.

[3] Shimada, M., An estimation of JERS-1's SAR Antenna Pattern using Amazon Rain Forest images, Proc. of the 1993 SAR Calibration Workshop, ESA WPP-048, ESTEC, Noordwijk, The Netherlands, pp. 185-208, September 1993.

[4] Ulander, L. M. H., Hawkins, R. K., Livingstone, C.E. and Lukowski, T.I., Absolute Calibration of the CCRS SAR, IEEE Trans. Geosci. and Rem. Sensing, Vol. 29, No. 6, 99.922-933, 1991.

[5] Curlander, J. C., Radiometric Calibration of the SIR-C System, in Progress in Imaging Sensors, Proc. ISPRS Symposium, Stuttgart, Sept. 1986, ESA SP-252, Nov. 1986.

[6] Wall, S.D. and Curlander, J. C., Radiometric Calibration Analysis of SIR-B Imagery, Int. J. Rem. Sensing, Vol. 9, No. 5, pp. 891-906, May 1988.

[7] Freeman, A., van Zyl, J. J., Klein, J. D., Zebker, H.A. and Shen, Y., Calibration of Stokes and scattering matrix format polarimetric SAR data, IEEE Trans. on Geoscience and Remote Sensing, vol. 30, No. 3, pp. 531-539, May 1992.

[8] Dubois, P. C., Evans, D. E. and van Zyl, J. J., Approach to Derivation of SIR-C Science Requirements, IEEE Trans. on Geoscience and Remote Sensing, Vol. 30, No. 6, pp. 1145-1148, November 1992.

[9] Holecz, F., Meier, E., Piesbergen, J. and Nuesch, D., Calibration of airborne and spaceborne SAR data, Proceedings of the 1994 SAR Calibration Workshop, September 1994, University of Michigan, USA, pp. 143-155.

[10] van Zyl, J. J., Calibration of Polarimetric Radar Images Using Only image Parameters and Trihedral Corner Reflector Responses, IEEE Trans. on Geoscience and Remote Sensing, Vol. GE-28, No.3, pp. 337-348, May 1990.

[11] Gray, A. L., Vachon, P. W., Livingstone, C.E. and Lukowski, T. I., Synthetic Aperture Radar Calibration Using Reference Reflectors, IEEE Trans. on Geoscience and Remote Sensing, VOI.GE-31, No. 3, May 1990, pp 374-383.

[12] Curlander, J. C. and McDonough, R. N., Synthetic Aperture Radar: Systems and Signal Processing, publ. John Wiley, 1991, pp. 291-294.

[13] Sheen, D. R., Freeman, A. and Kasischke, E. S. Phase calibration of Polarimetric SAR systems, IEEE Trans. on Geoscience and Remote Sensing, Vol. GE-27, No. 6, pp. 719-731, November 1989.